CHARACTERISTICS OF ACOUSTIC EMISSION SIGNALS FROM COMPOSITES

L. J. Graham and R. K. Elsley
Science Center, Rockwell International
Thousand Oaks, California 91360

ABSTRACT

Certain characteristics of acoustic emission (AE) signals from graphite-epoxy composite specimens were correlated last year with the mechanical behavior of the materials. Moisture degradation, which reduced the ultimate strength, resulted in a change in the AE amplitude distribution early in the loading history. Also, AE having distinct frequency spectral types tended to occur at or near singularities in the load curve. In order to transform those observations into a viable NDE tool, two things needed to be done: (1) develop a quicker and more objective method for extracting the pertinent correlations from the data, and (2) develop the statistical relationship between the AE characteristics and some mechanical strength parameter such as ultimate strength or remaining lifetime. The approach taken was to use computer pattern recognition techniques to analyze the data. A problem which was faced in this was the huge amount of data that are available in raw form from a single acoustic emission test. To reduce the amount of data, an intermediate feature extraction step was required and several ways of doing this, based on the prior work, were tried. As a result, the previous correlations between the acoustic emission signal characteristics and the mechanical condition of the composite were confirmed on a more objective basis. This now provides a tool for methodically studying and identifying the specific failure modes which occur in composite materials under various conditions.

Introduction

Certain characteristics of acoustic emission (AE) signals from graphite-epoxy composite specimens were correlated last year with the mechanical behavior of the materials. Moisture degradation, which reduced the ultimate strength, resulted in a change in the AE amplitude distribution early in the loading history. Also, AE having distinct frequency spectral types tended to occur at or near singularities in the load curve. Those observations were at best objective because of the broad range approach taken experimentally to identify useful correlations. In order to transform those observations into a viable NDE tool, two things need to be done: (1) develop quicker and more objective methods for extracting the pertinent correlations from the data, and (2) develop the statistical relationship between the AE characteristics and some mechanical strength parameter such as ultimate strength or remaining lifetime.

This year the work concentrated in these two areas. Particular characteristics of the AE signals were extracted in digital form and then processed on a minicomputer using special "pattern recognition" routines developed for this purpose.[1] The experimental methods were essentially the same as used last year except that the specimens were loaded in 4-point instead of 3-point bending to alleviate some minor problems experienced with the later configuration. Also, the specimen material was restricted to one type, the one designated as B-1 material last year,[2] and was chosen as being the most representative of actual structural materials. This was a graphite-epoxy laminate constructed by bonding several plies of the uncured material into sheets about 1/4 inch thick, with the graphite fibers all lying in the same direction. Its thermomechanical properties and details of its fabrication may be found in Reference 3. The features of the AE signals which were studied in detail were the distribution in time of the frequency spectral types and the amplitude distribution of the AE.

Frequency Spectral Types

In the previous work frequency spectral analysis was done by recording all the AE generated during a specimen test on a modified video tape recorder having a 3 MHz bandwidth and then doing a "stop action" spectral analysis manually on a representative number of individual AE signals. Pattern recognition by this method is all done in the head of the experimenter, and, due to the large amount of data involved, is necessarily fairly subjective. Typical results of this effort are shown in Figs. 12 and 13 of Ref. 2.

In the present work the same video tapes were played at full speed and a transient recorder (Biomation, Model 8100), under computer control, captures the first 40 μs of an emission at a 5 samples/μs rate. This waveform is stored in disk memory for later processing. In the work reported here, the computer/transient recorder captured 3000 emissions from a 25-minute, 3-point bending experiment on a piece of graphite-epoxy having event rates from several seconds per useable event to beyond the system's maximum capacity of 20 useable events/second. Due primarily to limitations in data transfer rates and in dynamic range, only about 1/8 the total number of AE events recorded were captured and stored by this method. They should, however, form a sufficiently large and unbiased sample of the total number to provide for valid classification if there are indeed different classes present.

In order to study general trends in the frequency spectra, we selected as features the maximum amplitude in each of several frequency bands, as well as the time of occurrence of the emission. The bands, 400 kHz wide and spaced 315 kHz apart, were chosen to be relatively broad so as to suppress structure due to sample and transducer resonances and the effect of emitter location on the fine structure of the spectrum. The maximum amplitude found in each band was used in an attempt to

remove the convolved effects of multiple signal paths.

In order that emissions with the same frequency content but different amplitudes be treated as similar, we normalized the amplitudes by the amplitude in the f = 0 frequency band, yielding 7 normalized frequency components. These 7 spectral components and the time of occurrence form an 8-element feature vector for each emission, so that each emission is represented by a point ("event") in an 8-dimensional vector space.

With this done, we can then start asking questions of the type, "What is the most common type of event?", by finding the event with the largest density of nearby points in the vector space defined above. Figure 1(a) shows the three highest density events during a part of the test. These events have the common "white noise" (WN) spectrum as defined in Ref. 2 (Fig. 12).

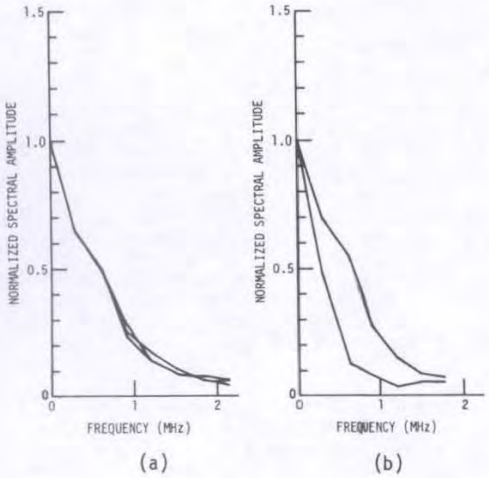

Figure 1. (a) Most common type of emission; (b) two well-separated categories of emissions.

We may further ask, "Are there distinct classes of events?", by looking for well-separated maxima in density. During much of the test, the answer is no. Except for the large maximum of density and some "foothills" probably due to statistical chance, there are so few, widely scattered events that it is not justified to call them separate classes. However, during one part of the test, there were a large number of emissions with very little high frequency energy. Here, the emissions separate easily into two regions of maximum density. Figure 1(b) shows the spectra of the highest density events in these two categories. Low frequency events occur during a 1-1/2 minute period immediately preceeding a period of massive emission event rate and substantial load drop. This type of event was called Type I in Ref. 2.

To see if certain emission classes correlate with the load history of the specimen, we have looked at the emissions occurring in the vicinity of a small sudden load drop early in the test. In order to see if there are types of events which, despite being too few in number to show significant maxima in the event density, are nonetheless informative about what was happening, we asked the question, "Which events are most unique to this time interval?", or in other words, which events are more likely to be found here than at other times during the test? Figure 2(a) shows the events in the vicinity of the small load drop with the highest uniqueness and Fig. 2(b) shows those with the lowest. There is a clear pattern of emissions with substantially more than the usual amount of energy in the 300-900 kHz region, and also even at 2 MHz. This is the high frequency Type II emission of Ref. 2. Even the least unique emissions have more high frequency energy than the more common emissions shown in Fig. 1(a).

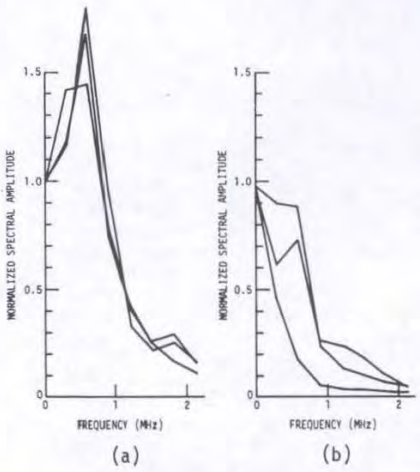

Figure 2. (a) Emissions most unique to the time period of a load drop; (b) emissions least unique to the load drop.

A similar technique can be used even without knowledge of an external feature such as the load. We may ask the question, "Which events are least uniformly distributed throughout the test?" Figure 3(a) shows the most nonuniformly distributed emissions during the first part of the test and Fig. 3(b) shows the least nonuniformly distributed ones. Again, emissions with more high frequency (or less low frequency) energy are the least uniformly distributed. Note the scale change in Fig. 3(a). This spectrum is like the Type III spectrum of Ref. 2.

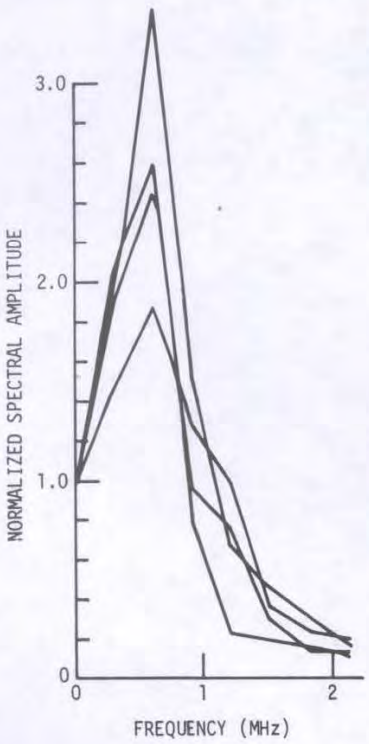

Figure 3. (a) Emissions most non-uniformly distributed throughout the test; (b) emissions least non-uniformly distributed throughout the test.

In these preliminary experiments we have demonstrated:

(1) That a minicomputer based data acquisition system can, in real time, capture a significant number of acoustic emission signals;

(2) That the minicomputer can rapidly classify them according to type, taking into account a variety of signal features; and

(3) That the computer can also discover relationships between the features of the emissions and what is known about the process going on in the specimen.

It is gratifying to find substantial agreement in the frequency spectral classifications made using this objective approach with those made previously by visual observations.

Amplitude Distribution Analysis

The previous amplitude distribution analyses had been done by recording the AE signals on the video tape recorder and then playing the tape back many times through a counter, each time changing the trigger level of the counter. This suffered two drawbacks; there were electrical noise spikes due to tape imperfections which were counted along with the recorded emission signals and the dynamic range was limited to that of the recorder. Both problems could be circumvented to some degree but the accuracy of the data suffered.

In the present work the first 200 μs of each AE signal was captured directly by the digital recorder during a specimen test at a 5 μs/sample rate, and the value of the maximum amplitude digital point and the time of occurrence of the emission event stored in the computer. To effectively increase the dynamic range of the measurements, both input channels of the digital recorder (Biomation, Model 8100) were utilized by taking the AE at two different signal levels from the amplifier chain. If the amplitude of an emission event exceeded the dynamic range of the digitizer on the most sensitive channel, its amplitude was determined by the value on the less sensitive channel times a constant multiplying factor. The dynamic range of the system, after reducing the quantization errors at the low amplitude end to < ½ dB and allowing for some range overlap, was 45 dB. At low AE event rates essentially all the emission events were captured and throughout an entire test of a specimen to fracture about 95% of the events were captured.

The specimens were bend bars 3.0 inches long with a square cross section of 0.250 inches. The surfaces were ground smooth, flat, and parallel and then a rectangular reduced cross section was formed at mid-length by cutting a 0.020 inch wide slit in from two opposite sides with a diamond saw leaving a 0.090 inch wide web. The specimens were loaded in bending so that a crack would advance down this web along its ¼ inch dimension. The specimen orientations with respect to the plate material were such that the maximum tensile stress due to bending was either along the fibers (L-direction) or transverse to them (T-direction) and the crack propagation direction was either through the plate thickness (S-direction) or in the T-direction. Specimens having LS, LT, TS, TL orientation

were tested, where the first letter designates the tensile stress direction and the second letter the crack propagation direction. An Instron machine crosshead speed of 0.005 cm/min was used throughout the study. Hydrothermal aging of the specimens was done by immersion in 100° C distilled water for various lengths of time.

Conventional AE count data were also recorded during the tests. Figure 4 shows typical loading curves for an unaged and a fully aged specimen. Also shown are the cumulative event count, N_E, cumulative emission count, N, and the incremental ratio of these two numbers over successive one-minute time intervals. This ratio is the average number of oscillations in each AE burst during the time interval and is a measure of the average amplitudes of the emission events. The trends are the same as determined previously[2] and show that the average amplitudes of the emission events in the aged material are lower throughout the loading history.

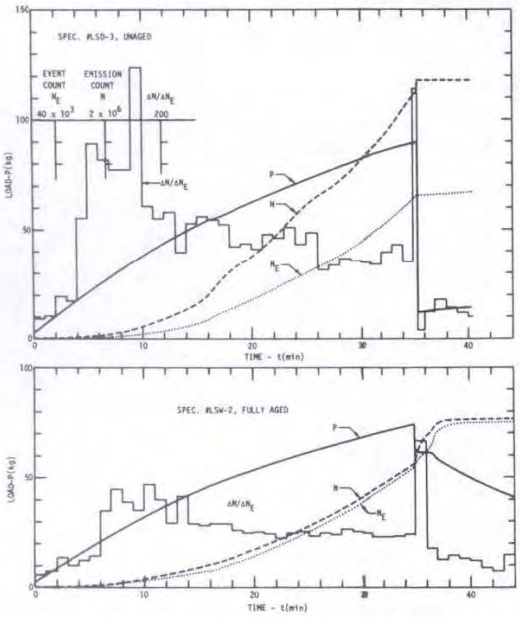

Figure 4. Typical load and acoustic emission vs. time histories for unaged and moisture degraded graphite-epoxy composite bend specimens.

The results of a second type of test are illustrated in Fig. 5. In these tests the load was cycled between successively higher load levels while continuously counting the number of emission events which occurred. These results indicate a depletion of AE generation sites with increasing load (Kaiser effect) which may be an important consideration when trying to establish the mechanical state of a composite structure at some point in its service life from the characteristics of the emission signals produced during proof loading. It will be shown in the following that information about the amount of moisture in the composite is contained in the cumulative amplitude distribution of the emission events throughout the loading history (as might also be implied from the results shown in Fig. 4). Further, only a small load increment above the previous high load is necessary to extract the information.

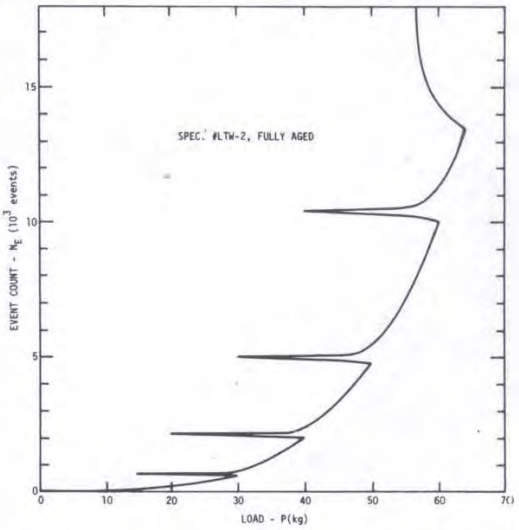

Figure 5. Load cycling results in a depletion of AE generation sites with increasing load (Kaiser effect).

Post-test analysis of the AE amplitude data which is stored in the computer can be done between any two points in the test either on the basis of event number or time. In Fig. 6 are the amplitude distributions of the first 500 emission events which occurred during the testing of unaged and fully aged LT-orientation specimens. For this orientation the direction of crack growth is across the fibers and parallel to the laminate plies. The key features of these distributions are that the emissions appear to fall in at least two distinct amplitude ranges and that the relative number of emissions in the low amplitude range is much greater for the fully aged material. These observations suggest the simultaneous occurrence of more than one AE generation mechanism and also a difference in activity of the mechanisms with aging. It is hypothesized that the mechanism which produces the low amplitude emissions is crazing of the epoxy matrix which is more predominant when the matrix is weakened by exposure to moisture. This hypothesis is unsupported at present, but regardless of the mechanism, if the shape of the amplitude distribution at the low amplitude end is related to moisture content of the composite, this phenomenological observation can be used to indicate the state of the material. Since the effect of moisture on ultimate strength is known,[3] this observation is also an indirect measure of that parameter.

The shapes of the amplitude distributions at the high amplitude end were found to be more sporadic, reflecting the statistical variability in the more macroscopic fracture processes with position in the material. Although there is believed to be a great deal of information about these processes contained in the amplitude data, no clear-cut correlations with the condition of the material has as yet emerged from the analyses.

Shown also in Fig. 6 is the amplitude distribution of the electronic amplifier noise and its amplitude relative to the amplitudes of the emission signals detected. Another way of illustrating this relationship is by the emission count rate produced by decreasing the counter trigger level (or increasing the amplitude gain) in successive 1 dB increments. At the trigger level used during the tests the event count rate was about 0.02 counts/sec, while lowering the trigger level in 1 dB increments produced count rates of 0.8, 14.0, and 106.2 counts/sec.

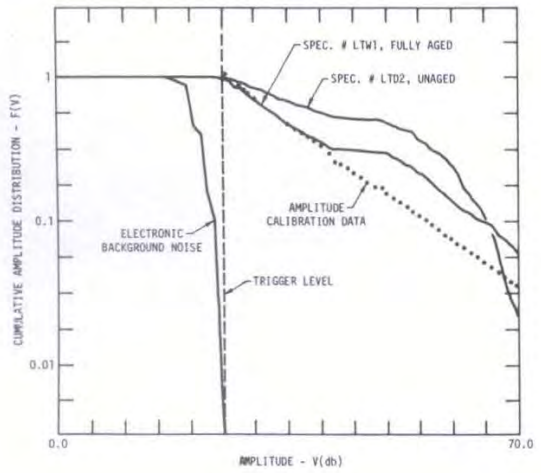

Figure 6. Typical cumulative amplitude distribution curves for unaged and fully aged specimens of the graphite-epoxy composite. Also shown is the electronic amplifier noise relative to the trigger level of the AE event detection circuitry and the system amplitude calibration data.

The remaining data in Fig. 6 are system amplitude calibration data obtained by injecting 50 μs duration bursts of 500 kHz signals at a repetition rate of 1 Hz into the input of the AE system preamplifier. These signals were treated as AE signals and their amplitudes measured and stored in the computer as the input amplitude was changed by 1 dB increments over a wide dynamic range. The pulse amplitudes in the computer were then plotted as if they had a specific power-law number distribution with the result shown in Fig. 6. It is seen that the plotted points all fall on a straight line, as they should, except for a slight deviation at the point of overlap of the two digital recorder channels. This deviation was considered insignificant to the results presented here and no effort was expended to find its cause.

The amplitude data for 14 specimens in the LT- and LS-orientations having various hydrothermal treatments were analyzed during various time periods of the tests. Additional specimens in the TL- and TS-orientations (crack propagation parallel to the fibers) failed in a brittle manner at loads which were 2-5% of the loads sustained by the other specimens. There were less than 50 AE produced during the loading of these specimens and so not much could be done in the way of data analysis.

A summary of the amplitude distribution data for the LS-orientation specimens is shown in Fig. 7. Here are plotted the slopes of the low amplitude portions of the amplitude distribution curves, such as shown in Fig. 6, as a function of water content of the composite determined gravimetrically. A relationship was clearly seen to exist between these two parameters at any stage in the loading history although the data for only four time periods are shown here.

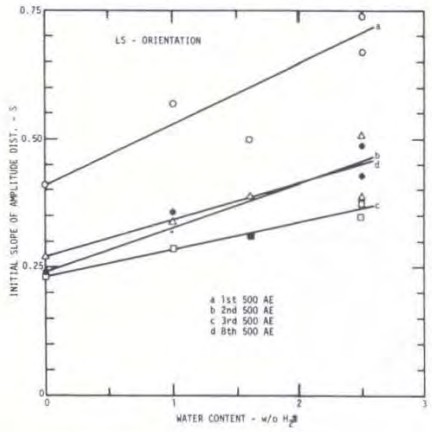

Figure 7. Dependence of the slope of the low amplitude end of the AE amplitude distribution on water content at various points in the loading of graphite-epoxy composite specimens in the LS-orientation.

A different result was found for the LT-orientation specimens as shown in Fig. 8. For these specimens the only correlation with the water content that was found was early in the loading history. At any time after the first few hundred emission events were generated, no dependence on water content was seen in the initial slope of the amplitude distribution.

We interpret this result as meaning that different fracture processes predominate in this load geometry. These specimens also failed at lower loads and with fewer AE generated at comparable times in the loading history than the LS-orientation specimens. These observations provide clues as to the identity of the fracture (AE) processes, but their identification, which was not a goal of this study, required considerably more effort.

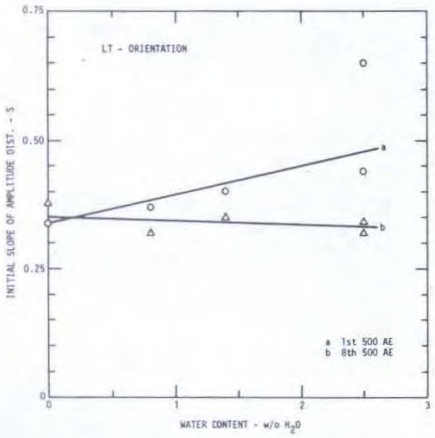

Figure 8. The LT-orientation bend specimens only showed a dependence of the amplitude distribution on water content early in the loading history.

Since the ultimate strength of a composite material has previously been shown to depend upon moisture content,[3] and a relationship has now been shown to exist between the moisture content and the initial slope of the AE amplitude distribution, then this AE parameter should also provide a measure of the ultimate strength of the material. Data for the limited number of specimens of this study which are plotted in Fig. 9 show just such a relationship. This result, which was anticipated from the previous qualitative observations, has now been established quantitatively, although a statistical validation is still required before an NDE useage can be established.

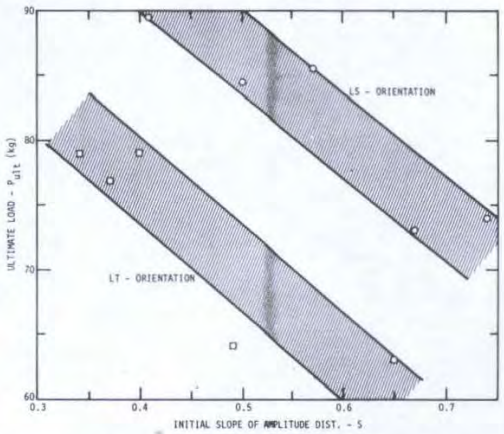

Figure 9. Relationship between the initial slope of AE amplitude distribution for the first 500 emission events and the ultimate fracture load for LS- and LT-orientation specimens with different amounts of hydrothermal aging.

Conclusions

In the current year's work it has been firmly established that at least two characteristics of the AE signals which are produced during the loading of a graphite-epoxy specimen contain information about the current mechanical state of the material. This information can then be used to estimate such parameters as the ultimate strength of the material or its remaining lifetime, if other information such as anticipated loading history is known. Emission signals having specific frequency spectral types were objectively correlated with singular points on the loading curve using computerized pattern recognition techniques. Also, the distribution in amplitude of the emission signals was quantitatively related to the moisture content of the composite material and to the ultimate strength of a given specimen. It was further shown that a minicomputer based data acquisition system can, in real time, capture a significant number of AE signals, rapidly and objectively classify them according to type taking into account a variety of signal features, and discover relationships between the features of the emissions and what is known about the process going on in the material.

Although we feel that these results are a significant advance toward providing an NDE tool for use during structural proof tests, more work needs to be done in relating the distinctive AE characteristics to specific microscopic fracture processes such as fiber fracture, matrix crazing, interlaminar matrix fracture, fiber-matrix debonding, and fiber pull-out. Identification of the statistical mix of these processes at any given time is considered to be essential to the useful interpretation of the acoustic emission data. We believe the tools are now available for doing this.

Acknowledgement

This research was sponsored by the Center for Advanced NDE operated by the Science Center, Rockwell International, for the Advanced Research Projects Agency and the Air Force Materials Laboratory under contract F33615-74-C-5180.

References

1. R. K. Elsley, Science Center, Rockwell International, deserves special credit for developing this software.

2. L. J. Graham, "Microstructure Effects on Acoustic Emission Signal Characteristics," in Interdisciplinary Program for Quantitative Flaw Definition, Special Report Second Year Effort, AFML Contract No. F33615-74-C-5180, Science Center, Rockwell International, August, 1976, pp. 297-320.

3. D. H. Kaelble and P. J. Dynes, "Methods for Testing Strength Degradation in Composites," (same report as Ref. 2), pp. 269-296.